

NASA/TM-2015-218808



# Application of the Refined Zigzag Theory to the Modeling of Delaminations in Laminated Composites

*Rainer M.J. Groh, and Paul M. Weaver  
University of Bristol, Bristol, United Kingdom*

*Alexander Tessler  
Langley Research Center, Hampton, Virginia*

October 2015

## The NASA STI Program Office . . . in Profile

Since its founding, NASA has been dedicated to the advancement of aeronautics and space science. The NASA Scientific and Technical Information (STI) Program Office plays a key part in helping NASA maintain this important role.

The NASA STI Program Office is operated by Langley Research Center, the lead center for NASA's scientific and technical information. The NASA STI Program Office provides access to the NASA STI Database, the largest collection of aeronautical and space science STI in the world. The Program Office is also NASA's institutional mechanism for disseminating the results of its research and development activities. These results are published by NASA in the NASA STI Report Series, which includes the following report types:

**TECHNICAL PUBLICATION.** Reports of completed research or a major significant phase of research that present the results of NASA programs and include extensive data or theoretical analysis. Includes compilations of significant scientific and technical data and information deemed to be of continuing reference value. NASA counterpart of peer-reviewed formal professional papers, but having less stringent limitations on manuscript length and extent of graphic presentations.

**TECHNICAL MEMORANDUM.** Scientific and technical findings that are preliminary or of specialized interest, e.g., quick release reports, working papers, and bibliographies that contain minimal annotation. Does not contain extensive analysis.

**CONTRACTOR REPORT.** Scientific and technical findings by NASA-sponsored contractors and grantees.

**CONFERENCE PUBLICATION.** Collected papers from scientific and technical conferences, symposia, seminars, or other meetings sponsored or co-sponsored by NASA.

**SPECIAL PUBLICATION.** Scientific, technical, or historical information from NASA programs, projects, and missions, often concerned with subjects having substantial public interest.

**TECHNICAL TRANSLATION.** English-language translations of foreign scientific and technical material pertinent to NASA's mission.

Specialized services that complement the STI Program Office's diverse offerings include creating custom thesauri, building customized databases, organizing and publishing research results ... even providing videos.

For more information about the NASA STI Program Office, see the following:

Access the NASA STI Program Home Page at <http://www.sti.nasa.gov>

E-mail your question via the Internet to [help@sti.nasa.gov](mailto:help@sti.nasa.gov)

Fax your question to the NASA STI Help Desk at 443-757-5803

Phone the NASA STI Help Desk at 443-757-5802

Write to:

NASA STI Help Desk  
NASA Center for AeroSpace Information  
7115 Standard Drive  
Hanover, MD 21076-1320

The use of trademarks or names of manufacturers in this report is for accurate reporting and does not constitute an official endorsement, either expressed or implied, of such products or manufacturers by the National Aeronautics and Space Administration.

Available from:

NASA Center for AeroSpace Information  
7115 Standard Drive  
Hanover, MD 21076-1320  
443-757-5802

## Abstract

*The Refined Zigzag Theory is applied to the modeling of delaminations in laminated composites. The commonly used cohesive zone approach is adapted for use within a continuum mechanics model, and then used to predict the onset and propagation of delamination in five cross-ply composite beams. The resin-rich area between individual composite plies is modeled explicitly using thin, discrete layers with isotropic material properties. A damage model is applied to these resin-rich layers to enable tracking of delamination propagation. The displacement jump across the damaged interfacial resin layer is captured using the zigzag function of the Refined Zigzag Theory. The overall model predicts the initiation of delamination to within 8% compared to experimental results and the load drop after propagation is represented accurately.*

## Nomenclature

RZT	Refined Zigzag Theory
ZZ	zigzag
CLA	Classical laminate analysis
FEM	Finite element method
VCCT	Virtual crack closure technique
GDQM	Generalized differential quadrature method
$k$	Layer number within laminate
$t^k$	Thickness of layer $k$
$u_x, u_z$	Displacements along x and z axes
$u_0, w$	Uniform displacements along x and z axes
$\theta, \psi$	Bending and zigzag cross-sectional rotations about

	negative y axis
$\phi^k$	Zigzag function of the Refined Zigzag Theory
$\sigma_x^k, \sigma_z^k$	Normal in-plane and normal transverse stresses within layer $k$
$\tau_{xz}^k, \gamma_{xz}^k$	Transverse shear stress and strain within layer $k$
$G_{xz}^k$	Transverse shear modulus of layer $k$
$T, S$	Tensile and shear strengths of the resin
$G_{II}$	Critical energy release rate in Mode II
$\delta^k$	Displacement jump across layer $k$
$\tau_{xzc}^k$	Critical transverse shear stress within layer $k$ at delamination initiation
$\delta_c^k, \delta_f^k, \delta_{\max}^k$	Critical displacement jump at delamination initiation, final displacement jump at layer separation, and maximum displacement jump throughout loading history across layer $k$
$d^k$	Damage variable of layer $k$
$\sigma_{ij}^k, \epsilon_{ij}^k$	Stress and strain tensors of layer $k$
$E_{ijmm}^k$	Hookean elasticity tensor of layer $k$
$A_{ij}^{(n)}$	The $n^{\text{th}}$ derivative weighting matrix of the differential quadrature method

# 1. Introduction

Composite materials, owing to their favorable specific strength and specific stiffness properties, are a key technology for reducing the weight and improving performance of future aerospace vehicles. An important aspect in designing advanced composite structures is understanding how these materials fail under service loads. The failure behavior of laminated composite structures is often governed by complex interactions of multiple intralaminar failure mechanisms, e.g. matrix cracking and fiber fracture, as well as interlaminar damage such as delamination. The damage mechanism that influences the load redistribution from failed to unfailed material is typically direction-dependent and is often governed by geometric and/or constitutive non-linearities. Furthermore, advanced composites maintain considerable load-carrying capability past the initiation of the first failure site. This behavior arises because the failed/damaged material has the capability to unload and redistribute the internal loads to the remaining undamaged material, and because adjacent plies can create a constraining effect that localizes the damage. Under these circumstances, initial first-ply failure criteria such as the maximum strain, maximum stress, Tsai-Wu, Tsai-Hill or Hashin-Rotem criteria [1] may only provide conservative estimates of laminate strength. As a result, progressive damage models that model the degradation of material and the growth of damage until final failure have received much attention over the past 30 years [2].

For the sake of simplicity, the study of damage in composites is often split into separate analyses of intralaminar damage and delaminations, even though these mechanisms may interact. Material degradation models such as ply-discounting and continuum damage models are two methods for modeling intraply damage. Ply-discounting techniques use heuristic knock-down factors to degrade certain material properties of a ply when failure is detected using an interactive or non-interactive initiation criterion. Both the magnitude of the knock-down factor and the degraded engineering constants may be failure-mode dependent. In continuum-damage models, the material properties are gradually degraded as a function of an evolving internal state variable, such as strain, that models the accumulation of damage. Therefore, these techniques are less heuristic than ply-discounting techniques and may be derived using thermodynamically consistent relations [3].

Traditionally, the study of delaminations is split into two distinct phenomena: the initiation of the crack and the ensuing propagation, where the latter is based on formulae of a pre-existing crack. The virtual crack closure technique (VCCT) proposed by Rybicki and Kanninen [4] is often used for predicting delamination growth. However, in the finite element method (FEM), VCCT results are dependent on the mesh in front of the crack tip and a pre-defined location of a crack is required. Unfortunately, the exact location and size of this initial crack may be difficult to determine *a priori*.

One approach to overcome the limitations of VCCT is the use of interfacial decohesion elements. The aim of the decohesion elements is to model the quasi-brittle process zone that appears in the wake of the crack tip. Usually, propagation of a crack does not cause immediate separation of two layers, whereby the residual cohesion may occur due to fiber bridging across the crack, or sliding friction between the surfaces. A cohesive law relates the three tractions acting on the two fracture surfaces with the associated interfacial displacement jumps [5]. For example, a cohesive law for Mode I relates the direct normal traction to normal displacement jumps, while the laws for Mode II and Mode III relate the shear tractions to in-plane displacement jumps. In the FEM, the cohesive zone is most often implemented using user-defined cohesive elements to represent the inter-ply resin that separates the actual plies modeled using full three-dimensional (3-D) elements. However, the high computational cost of non-linear 3-D finite element models restricts the use of cohesive elements to pre-determined failure sites and prohibits the use of these models for preliminary design studies.

Higher-order equivalent single-layer models are an attractive compromise between reduced computational cost and accurate 3-D stress fields. In this respect, the Refined Zigzag Theory (RZT) developed by Tessler et al. [6-8] is a potential candidate as it has been shown to accurately model the stretching and

bending of laminated beams and plates, even when the material properties of individual plies vary by orders of magnitude [9]. This feature makes the RZT applicable to explicitly modeling finite interfacial resin layers in pristine and degraded (damaged) states. Currently, only one attempt has been made to use RZT to model delamination damage in laminated composites by applying a continuum damage model to an interfacial resin layer [10]. In the current paper, the concept of cohesive zones is applied within the framework of RZT to model delaminations in beams.

## 2. Approach

In RZT, the displacement field of a beam is given in terms of four functional unknowns,

$$u_x^k(x, z) = u_0(x) + z\theta(x) + \phi^k(z)\varphi(x) \quad (1)$$

$$u_z(x) = w(x) \quad (2)$$

where  $u_0$  is a uniform axial (stretching) displacement,  $\theta$  is the bending rotation,  $\varphi$  is the zigzag rotation, and  $w$  is the transverse displacement. The zigzag function  $\phi^k$  in ply  $k$  is derived from the ratio of the local transverse shear modulus  $G_{xz}^k$  to the equivalent transverse shear modulus of the whole laminate (see [6]). The zigzag function models the occurrence of slope changes in the axial displacement field  $u_x^k$  at layer interfaces that occur because of differences in the transverse shear moduli of adjacent layers (Figures 1-5).

The displacement field assumption is used alongside the principle of virtual displacements to derive a set of variationally consistent governing field equations and boundary conditions [6] that are solved for the four functional unknowns. In RZT, the axial stress field  $\sigma_x$  is derived from the kinematic equations and constitutive relations. The transverse shear stress  $\tau_{xz}$  and transverse normal stress  $\sigma_z$  are derived in a post-processing step by integrating the axial stress in Cauchy equilibrium equations for greater accuracy.

The present approach of modeling delaminations using RZT is best explained using an example. Consider a  $[0_{12}/90/0_{12}]$  laminated beam, simply supported at both ends and loaded at mid-span by a transverse point load. As the Young's and shear moduli  $E_x$  and  $G_{xz}$  of the 90-degree ply are degraded, the displacement field transitions from purely linear to a pronounced zigzag shape through the thickness. When the 90-degree ply is fully damaged, two observations can be made regarding the laminate behavior:

- The axial displacement is fully reversed throughout the  $0_{12}$  sublaminates, i.e. tension and compression occur within each sublaminate. This means the sublaminates are bending independently as the 90-degree ply provides little structural connection (Figures 6-7).
- Due to the pronounced shear deformation throughout the 90-degree ply, the  $0_{12}$  sublaminates move relative to each other, i.e. there is a displacement jump between the bottom interface of the upper sublaminate and the top interface of the lower sublaminate (Figure 8).

Thus, the approach presented herein is to insert layers of isotropic resin material between the composite plies and use a cohesive zone approach to model the interfacial degradation. In this manner, Mode II shearing fracture is modeled for beams, and both shearing Modes II and III are modeled for plates. Note that because RZT is based on an equivalent single-layer formulation, the material properties of the interfacial resin layers cannot be degraded absolutely to zero in order to maintain numerical stability when solving the governing equations. Therefore, in this paper, a fully damaged resin layer has material

properties that have been degraded by 12 orders of magnitude, resulting in negligible properties compared to the undamaged composite plies (Figures 6b and 7b).

It is not possible to implement the cohesive zone concept directly within RZT because the commonly used cohesive element within FEM is not a full 3-D element based on continuum mechanics. Rather, it represents the interfacial surfaces that are created as the crack propagates and therefore defines the constitutive relation between the three surface tractions (one normal and two shearing) and the three components of the interfacial displacement jump (Figures 9-10). As there is no unique relation between stresses and displacements in 3-D elasticity, an arbitrary constant of proportionality  $K_p$  is defined for conventional cohesive elements used in 3-D FEM discretizations. Conversely, each ply within RZT requires a constitutive relation between the stress and strain tensors by using the elasticity tensor as a constant of proportionality. Thus, a pre-defined relation exists between stresses and strains based on the isotropic material properties of the resin. To remedy the inconsistency between these two approaches, the method proposed by Fan et al. [11] is adapted to RZT in this paper (Figure 11). The interfacial shearing displacement jump  $\delta^k$  is derived from

$$\delta^k = t^k \bar{\gamma}_{xz}^{-k} \quad (3)$$

where  $t^k$  is the thickness of the resin layer  $k$  and  $\bar{\gamma}_{xz}^{-k}$  is the average shear strain within the resin layer. This approach is equivalent to defining the initial penalty stiffness  $K_p$  of a cohesive element within a 3-D FEM discretization to be

$$K_p = \frac{G_{xz}}{t} \quad (4)$$

as used by several authors in the literature [5], and where  $t$  is the thickness of the interfacial resin layer.

Thus, in the framework presented herein, thin resin layers of 10 $\mu$ m thickness are modeled as explicit isotropic layers between composite plies, and the axial stress  $\sigma_x$ , transverse shear stress  $\tau_{xz}$  and transverse normal stress  $\sigma_z$  within this layer are calculated from the RZT governing equations. Damage initiation within a resin layer is defined when the quadratic failure criterion

$$e = \frac{\langle \sigma_x^2 \rangle + \langle \sigma_z^2 \rangle}{T^2} + \frac{\tau_{xz}^2}{S^2} \quad (5)$$

exceeds unity, where  $T$  and  $S$  are the tensile and shear strengths of the resin, respectively. Macaulay brackets  $\langle \dots \rangle$  are used as compressive normal tractions do not contribute to the onset of delamination. At the point of failure initiation, the critical interfacial shearing displacement jump  $\delta_c^k$  is calculated from the critical transverse shear stress  $\tau_{xzc}^k$  within the resin layer,

$$\delta_c^k = t^k \frac{\tau_{xzc}^k}{G_{xz}^k} \quad (6)$$

Thus, the damage variable  $d^k$  at a point within a damaged resin layer is found using the usual bi-linear cohesive law [5],

$$d^k = \frac{\delta_f^k (\delta_{\max}^k - \delta_c^k)}{\delta_{\max}^k (\delta_f^k - \delta_c^k)} \quad (7)$$

where  $\delta_{\max}^k$  is the maximum interfacial shearing displacement jump that has occurred during the load history and  $\delta_f^k$  is the final interfacial displacement jump at which complete decohesion occurs. The value of  $\delta_f^k$  is found from the fact that the area under the cohesive traction-displacement curve is equal to the critical surface fracture energy  $G_{Ic}$ . Thus,

$$\delta_f^k = \frac{2G_{Ic}}{\tau_{xz}^k} \quad (8)$$

Once the damage variable  $d^k$  at a specific mesh point within a resin layer is determined, all engineering constants within the elasticity tensor are degraded

$$\sigma_{ij}^k = (1 - d^k) E_{ijmn}^k \varepsilon_{mn}^k \quad (9)$$

As a result, the internal loads are redistributed within the laminate via two mechanisms. First, the reduction of the axial and transverse shear moduli causes a load redistribution to the surrounding material. Second, degradation of the transverse shear modulus  $G_{xz}$  locally increases the zigzag function such that the sublaminates above and below a damaged interface can move relative to each. Without the added functionality of the zigzag function within RZT this mechanism would not occur.

Accurate derivations of the transverse stresses  $\tau_{xz}$  and  $\sigma_z$  using Cauchy equilibrium equations in a post-processing step depend on accurate differentiation of the axial stress field  $\sigma_x$ . In the classic weak-form FEM, the recovery of these gradients from the element shape functions can lead to the propagation of numerical noise. Discrepancies in the transverse stress profiles lead to errors in the damage initiation location. This point is important as small perturbations in the initial damage site can lead to different post-damage behavior.

In this paper, the strong-form FEM based on elemental shape functions derived from the general differential quadrature method (GDQM) is used to discretize and solve the problem numerically. In GDQM, the governing differential equations are converted into algebraic ones by using a matrix differential operator that is derived from Lagrange polynomials (Figure 12). In this manner a derivative of a function can be replaced by a linear weighted sum of all functional values within the discretization domain, i.e.

$$\frac{\partial^n f(x_i)}{\partial x^n} = A_{ij}^{(n)} f(x_j) \quad i = 1, 2, \dots, N \quad (10)$$

where  $A_{ij}^{(n)}$  is the  $n^{\text{th}}$  derivative weighting matrix. Thus, the domain is discretized into finite GDQM elements that are based on higher-order polynomial shape functions giving an *hp-type* FEM. As the governing equations are solved in the strong form, derivatives of the axial stress  $\sigma_x$  can be calculated accurately and efficiently using the GDQM weighting matrixes [12], and numerical noise in the derivation of transverse stresses  $\tau_{xz}$  and  $\sigma_z$  is minimized.

Due to the degradation of material properties, a non-linear solver is required. In this work, an iterative-incremental Newton-Raphson solver was implemented in MATLAB® to solve the strong-form GDQM equations. Thus, the incremental equilibrium equation

$$K(C_{(t+\Delta t,i)}^k)\Delta u_{(t+\Delta t,i)} = F_{(t+\Delta t,i)} - f_{(t+\Delta t,i)} = R_{(t+\Delta t,i)} \quad (11)$$

is solved until the residual vector  $R$  is lower than the convergence tolerance of  $10^{-4}$ . In the equation above,  $K(C_{(t+\Delta t,i)}^k)$  is the tangent stiffness matrix at load step  $(t + \Delta t, i)$  in the  $i^{\text{th}}$  iteration, and  $C^k$  equals to the material stiffness matrices of the different plies in the laminate. The difference between the known external force vector  $F$  and internal force vector  $f$  gives the residual  $R$ , while  $\Delta u_{(t+\Delta t,i)}$  is the incremental displacement vector at the  $i^{\text{th}}$  iteration. Before damage occurs, the material stiffness matrices of all resin layers are equal to their pristine values  $C_0^k$ . However, upon damage initiation within a resin layer, the engineering constants that define  $C^k$  are degraded at the damaged locations according to Eq. 9.

### 3. Discussion and Conclusions

The approach presented herein was used to predict the failure behavior of several cross-ply beams. For this purpose, the experimental results of the three-point bend test in the experimental study by Yuen et al. [13] were used for comparison purposes. In these tests, a single 90-degree ply was inserted at different locations throughout the thickness of a  $[0_{24}]$  laminate (Figure 13). The more compliant 90-degree ply acts as a weak interface to initiate delamination without the need for manufacturing a specimen with a preexisting crack. This load case is dominated by Mode II fracture and therefore presents a good validation study for the presented Mode II RZT damage model.

In the present RZT model, interfacial damage is modeled by inserting thin 10 $\mu\text{m}$  isotropic resin layers on either side of the 90-degree ply using the resin properties given by Yuen et al. [13]. The results in Figures 14 and 15 indicate that the pre-damage behavior and post-damage load drop is modeled accurately by the RZT damage model. The load at which the first load drop occurs is predicted to lie within 8% of the experimental results for all cases considered (see the tables on p. 18). The location of the initial delamination site is predicted most accurately when the load pin used in the experimental studies is small (case S-40-1/2). This response happens because the contact area of the load pin was ignored in the computational model by applying a concentrated load. However, in all five cases, the size of the delamination after the first load drop is predicted accurately by the RZT model (Figures 16 and 17).

In conclusion, the general trends of delamination initiation and propagation are modeled to adequate accuracy ( $\sim 10\%$  error) given the low computational cost of the underlying RZT equivalent single-layer beam model. The most accurate predictions, compared to the experimental results, occur when the load pin contact area in the experiments was small, as this contact area is not modeled explicitly herein.

Currently, the resin layer is only modeled explicitly on either side of the 90° layer, as this is known to be the weak location. Further work needs to focus on placing resin layers within the 0° blocks to make sure that the model does not predict delamination here.

The bending load case considered herein results in fracture behavior that is Mode II dominated. Thus, the present investigation can serve as a foundation for applying the methodology to end-notched flexure specimens and general laminates with off-axis fiber angles, and these load cases will be the topic of future work. The present approach should also be extended to the analysis of plates to analyze both Mode II and Mode III fracture. On the other hand, in-plane mode I-dominated load cases will be modeled less

accurately with the present framework, but this can be remedied by incorporating transverse normal ZZ effects in the underlying RZT formulation.

Finally, the cohesive zone approach presented herein is only one possible application of RZT to damage modeling. A large number of continuum damage models for interply and intraply damage have been published in the literature, and any one of these can be explored within the general framework presented herein. Perhaps, intraply and interply damage models can be combined within the presented framework to account for both modes of failure simultaneously.

## Acknowledgements

This work was supported by the Engineering and Physical Sciences Research Council through the EPSRC Centre for Doctoral Training in Advanced Composites for Innovation and Science [grant number EP/G036772/1]. The authors would also like to thank NASA Langley Research Center for hosting Rainer M.J. Groh at the National Institute of Aerospace under the Advanced Composites Project.

## References

- [1] J. Echaabi, F. Trochu, and R. Gauvin. Review of failure criteria of fibrous composite materials. *Polymer Composites*, 17(6):786-796, 1996.
- [2] M.R. Garnich, and V.M.K. Akula. Review of degradation models for progressive failure analysis of fiber-reinforced polymer composites. *Applied Mechanics Reviews*, 62(1):1-33, 2009.
- [3] P. Maimi, P.P. Camanho, J-A. Mayugo, and C.G. Davila. A thermodynamically consistent damage model for advanced composites. *Technical Report NASA/TM-2006-214282*, 2006.
- [4] E.F. Rybicki, and M.F. Kanninen. A finite element calculation of stress intensity factors by a modified crack-closure integral. *Engineering Fracture Mechanics*, 9:931-938, 1977.
- [5] P.P. Camanho, C.G. Davila, and M.F. de Moura. Numerical simulation of mixed-mode progressive delamination in composite materials. *Journal of Composite Materials*, 37(16):1415-1435, 2003.
- [6] A. Tessler, M. Di Sciuva, and M. Gherlone. Refinement of Timoshenko beam theory for composite and sandwich beams using zigzag kinematics. *Technical Report NASA/TP-2007-215086*, 2007.
- [7] A. Tessler, M. Di Sciuva, and M. Gherlone. A refined zigzag beam theory for composite and sandwich beams. *Journal of Composite Materials*, 43(9): 1051-1081, 2009.
- [8] M. Di Sciuva, M. Gherlone, and A. Tessler. A robust and consistent first-order zigzag theory for multilayered beams. “*Advances in Mathematical Modelling and Experimental Methods for Materials and Structures: The Jacob Aboudi Volume*” (GILAT R.; BANKS-SILLS L.), Springer Publishing (USA), pp.255-268, ISBN: 9048134668, 2009.
- [9] R.M.J. Groh, and P.M. Weaver. On displacement-based and mixed-variational equivalent single-layer theories for modelling highly heterogeneous laminated beams. *International Journal of Solids and Structures*, 59:147-170, 2015.
- [10] A. Eijo, E. Onate, and S. Oller. A numerical model of delamination in composite laminated beams using the LRZ beam element based on the refined zigzag theory. *Composite Structures*, 104:270-280, 2013.

- [11] C. Fan, P.-Y. Ben Jar, and J.J. Roger Cheng. Cohesive zone with continuum damage properties for simulation of delamination development in fiber composites and failure of adhesive joints. *Engineering Fracture Mechanics*, 75:3866-3880, 2008.
- [12] F. Tornabene, N. Fantuzzi, E. Viola, and R.C. Batra. Stress and strain recovery for functionally graded freeform and doubly-curved sandwich shells using higher order equivalent single-layer theory. *Composite Structures*, 119:67-89, 2015.
- [13] S. Yuen, C. Fan, T. Kuboki, P.-Y. B. Jar, T.W. Forest, and J.J.R. Cheng. Delamination resistance of fiber-reinforced polymers (FRP) under transverse loading - Criteria for onset of delamination. *ANTEC 2004 - Annual Technical Conference Proceedings. 2.* 1374-1378.
- [14] Gherlone, M. On the use of zigzag functions in equivalent single-layer theories for laminated composite and sandwich beams: A comparative study and some observations on external weak layers. *Journal of Applied Mechanics*, 80:1-19, 2013.
- [15] P.P. Camanho, C.G. Davila, and D.R. Ambur. Numerical simulation of delamination growth in composite materials. NASA/TP-2001-211041, 2001.
- [16] Q. Yang, and B. Cox. Cohesive models for damage evolution in laminated composites. *International Journal of Fracture*, 133:107-137, 2005.

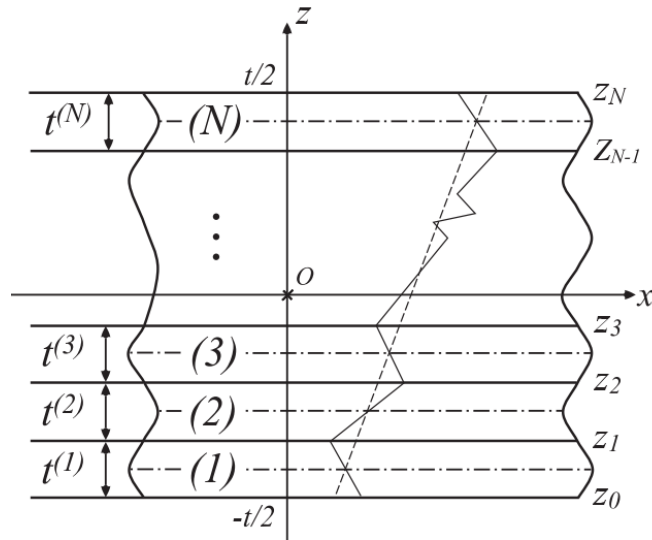


Fig. 1 Arbitrary stacking sequence of  $N$  layers with notation of layer thicknesses and interface locations. The dashed line represents the continuous through-thickness deformation of CLA, whereas the solid, piecewise continuous line shows the ZZ displacement field.

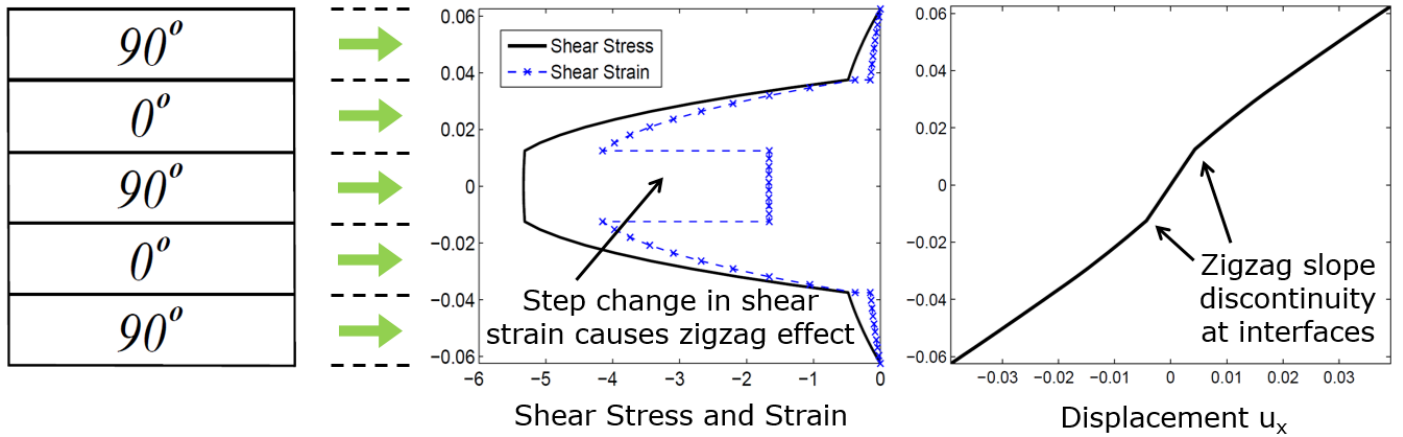
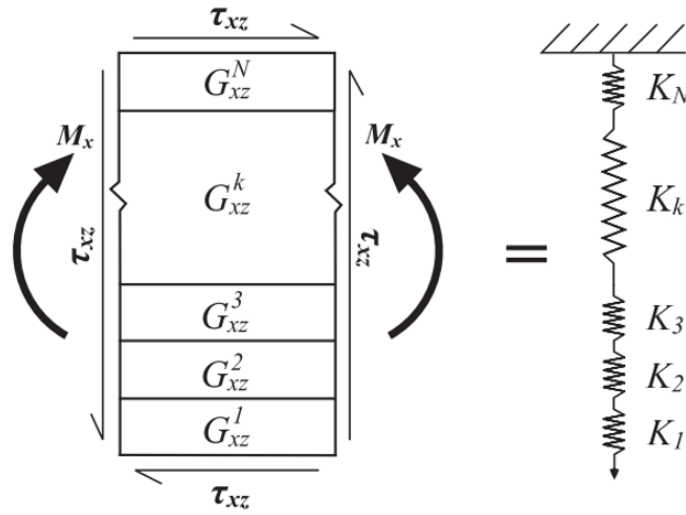


Fig. 2. The ZZ effect is driven by differences in transverse shear moduli of adjacent layers, e.g.  $0^\circ$  and  $90^\circ$  layers. As transverse shear stresses are continuous at layer interfaces, the transverse shear strains are different at the interfaces of distinct layers, and therefore cause a piecewise change in  $\frac{\partial u_x}{\partial z}$ .



Equivalent spring stiffness

$$G = \left[ \frac{1}{t} \sum_{k=1}^N \frac{t^{(k)}}{G_{xz}^{(k)}} \right]^{-1}$$

Fig. 3 In the RZT beam theory, the Timoshenko beam displacement field is enhanced via a ZZ variable multiplied by a piecewise continuous ZZ function  $\phi^k(z)$ . This function is derived by assuming that the transverse shear behavior of the laminate can be modeled as a system of springs-in-series with an equivalent spring stiffness  $G$ .

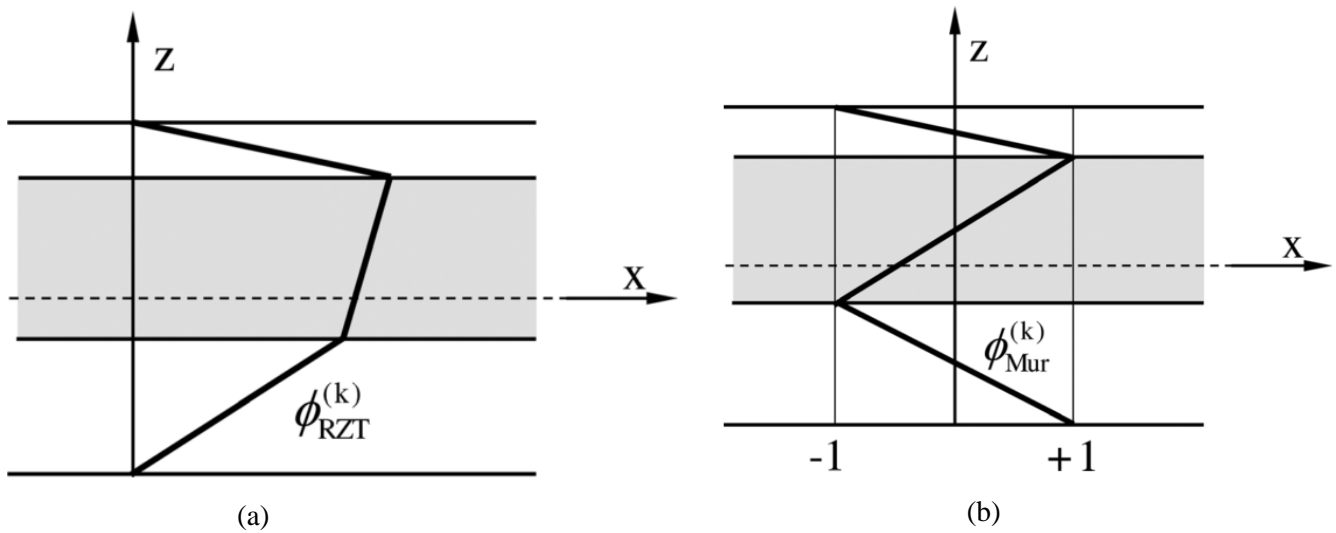


Fig. 4 Differences between the RZT ZZ function in (a) and Murakami's ZZ function in (b). Murakami's ZZ function takes arbitrary values of  $\pm 1$  at layer interfaces. The RZT ZZ function is zero at the top and bottom surfaces but is based on the actual material properties (adapted from [14]).

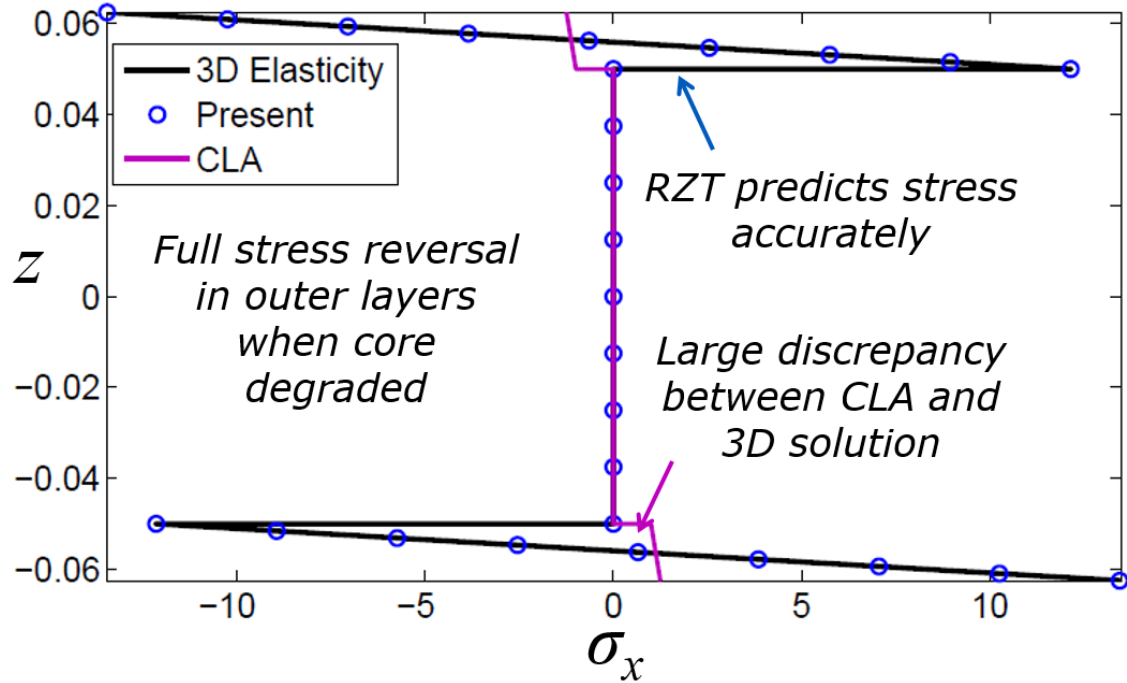
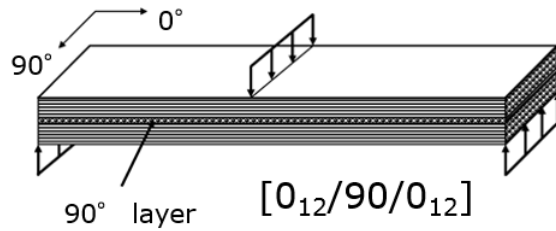
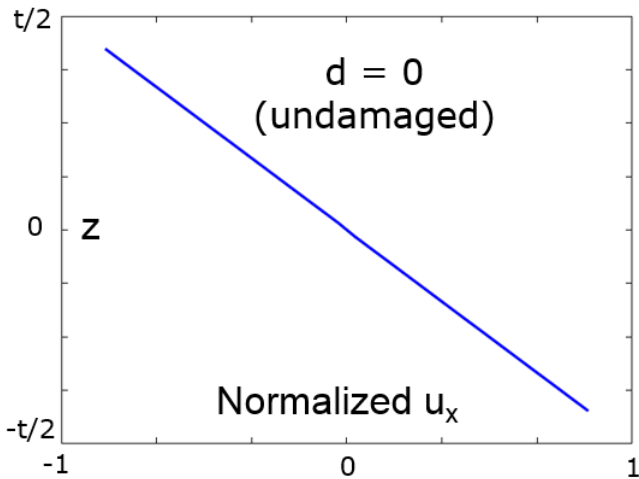


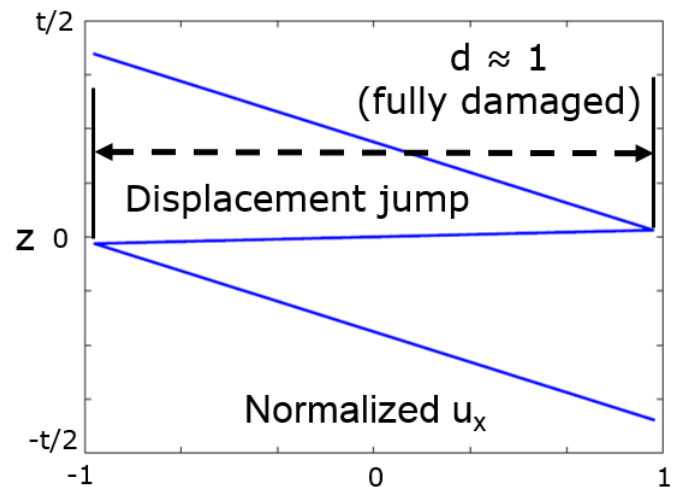
Fig. 5 The RZT ZZ function can model laminates where different layer have material properties that vary by orders of magnitude. For example, a sandwich beam with stiff face layers and heavily degraded central core, shows a full stress reversal in the outer layers when loaded in bending, i.e. the outer layers are both in compression and tension. CLA cannot account for this behavior.



$$(E_x, G_{xz}) = (1 - d) \cdot (E_x, G_{xz})$$

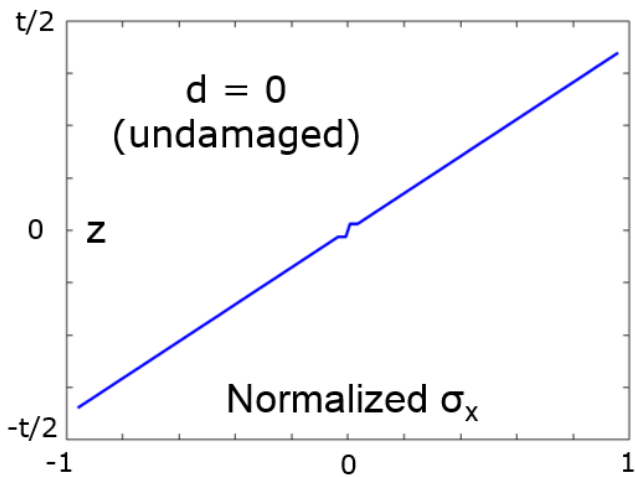


(a)

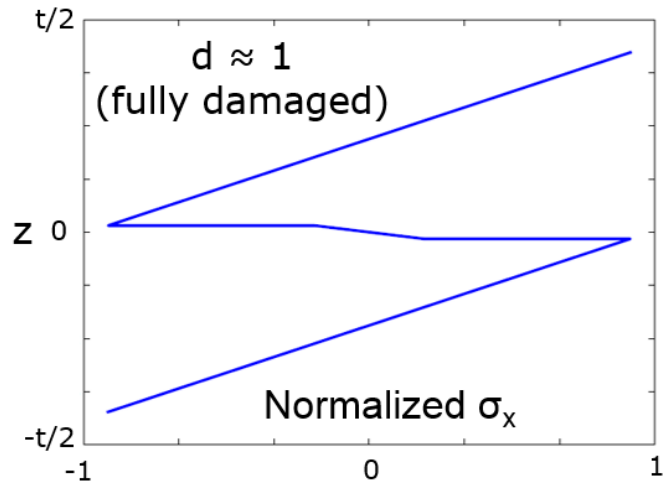


(b)

Fig. 6. A  $[0_{12}/90/0_{12}]$  laminated beam in three-point bending where the stiffness tensor of the central  $90^\circ$  layer is degraded using the damage parameter  $d$ . When the central layer is undamaged in (a), the displacement field is linear as predicted by CLA. However, when the central layer is damaged in (b), a displacement jump occurs, which is modeled via the RZT ZZ function.



(a)



(b)

Fig. 7 Similarly, the axial stress field throughout the laminate thickness changes from a classic solution when the central layer is undamaged in (a) to a non-classical stress field with stress reversal in the blocks of  $0^\circ$  when the central layer is damaged in (b).

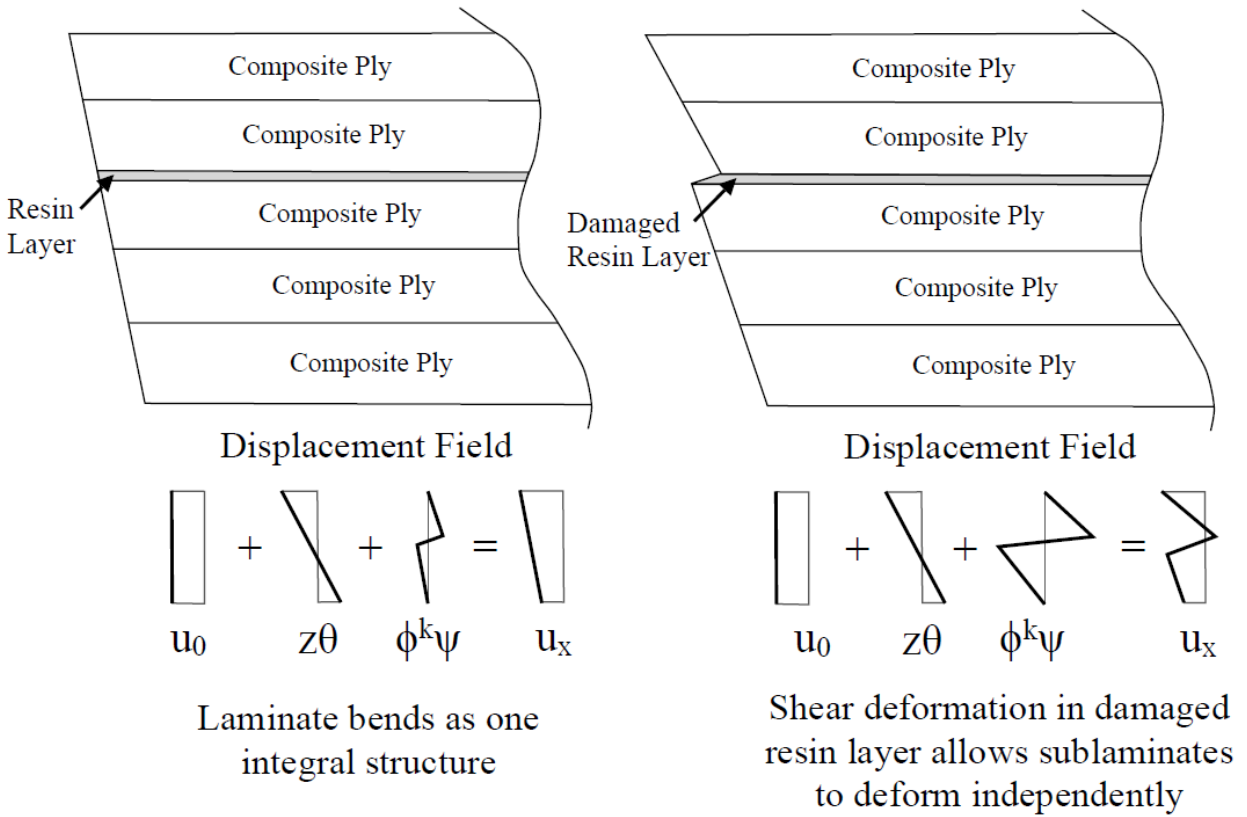


Fig. 8 Schematic showing how the RZT beam model can be used to explicitly model the thin interfacial resin layers. The resin layer is modeled using isotropic material properties, and when undamaged does not influence the linear bending displacement field. When damaged, the resin layer allows the two sublaminates to slide (shear) over each other, and this is modeled using the ZZ function.

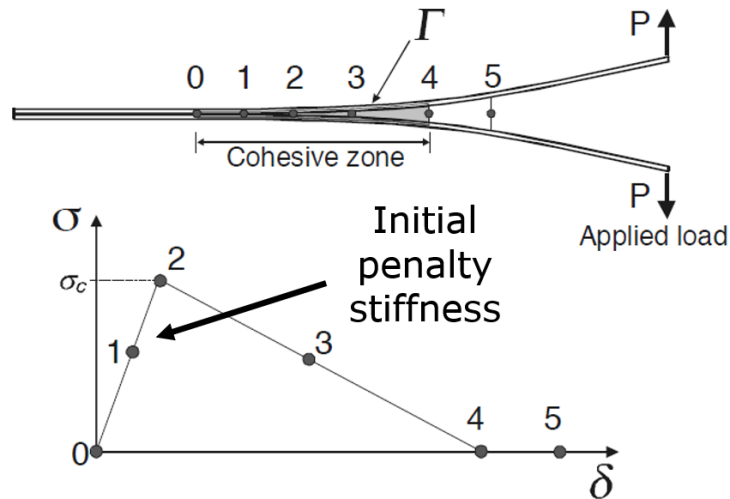


Fig. 9 Schematic showing the concept of a brittle Mode I cohesive zone in a double cantilever beam test. The cohesive zone is modeled via a bi-linear traction-displacement law of fictitious initial stiffness. When a critical stress limit is reached the layer is damaged, and stress is offloaded onto other parts of the structure (adapted from [15]).

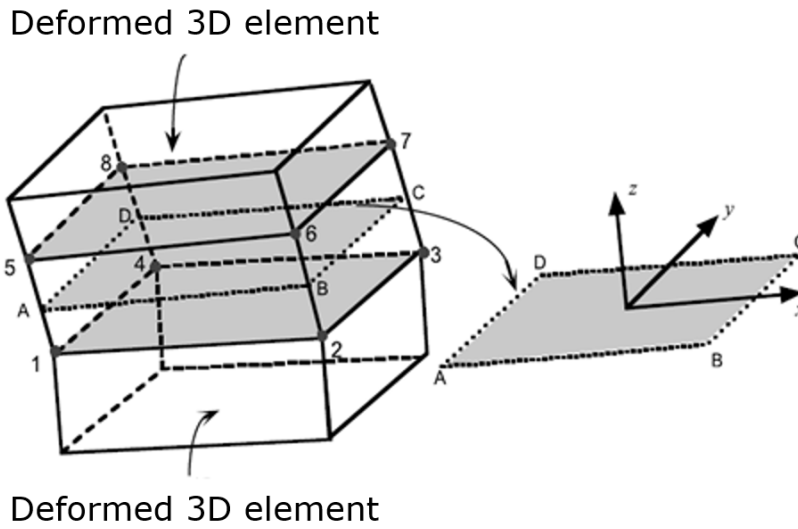


Fig. 10 Schematic diagram of a 3D cohesive finite element embedded between two 3D continuum finite elements. The cohesive element is not governed by the classic stress-strain constitutive tensor but by a pre-defined traction-displacement law (adapted from [16]).

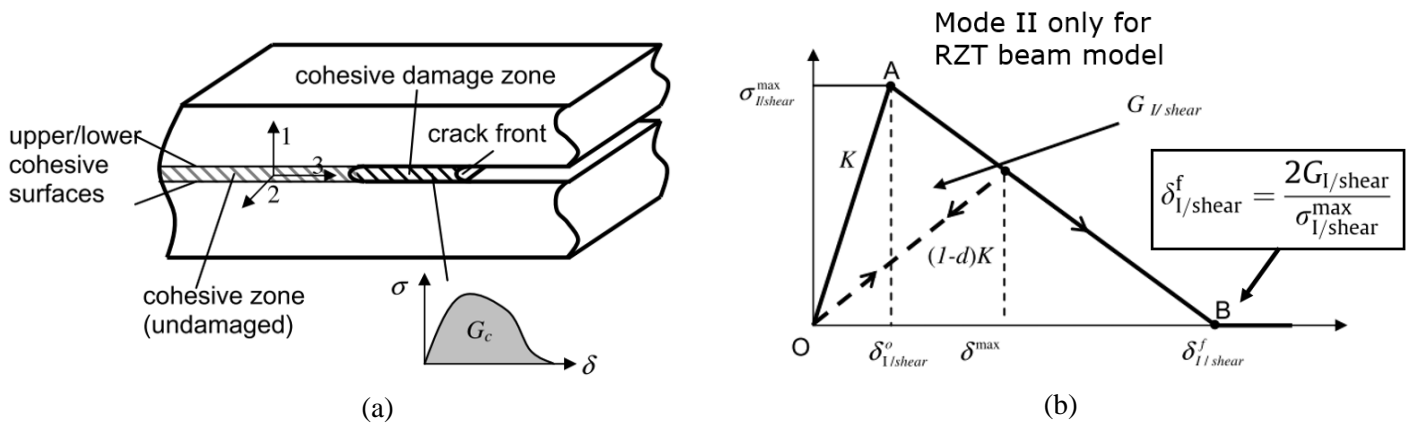


Fig. 11 Schematic showing the implementation of the cohesive zone damage model of Fan et al. [11]. Here, the resin rich interfacial layer is not modeled using a classical cohesive element with a traction-displacement constitutive model, but rather using the classical stiffness tensor, i.e. a stress-strain law. Thus, the stiffness tensor is degraded directly when damage occurs. The displacement jump across the interface in (b) is derived from the thickness of the resin layer and the transverse shear strain across it. The continuum damage model approach means that this cohesive zone model can readily be implemented in a RZT beam model to analyze Mode II fracture (adapted from [11]).

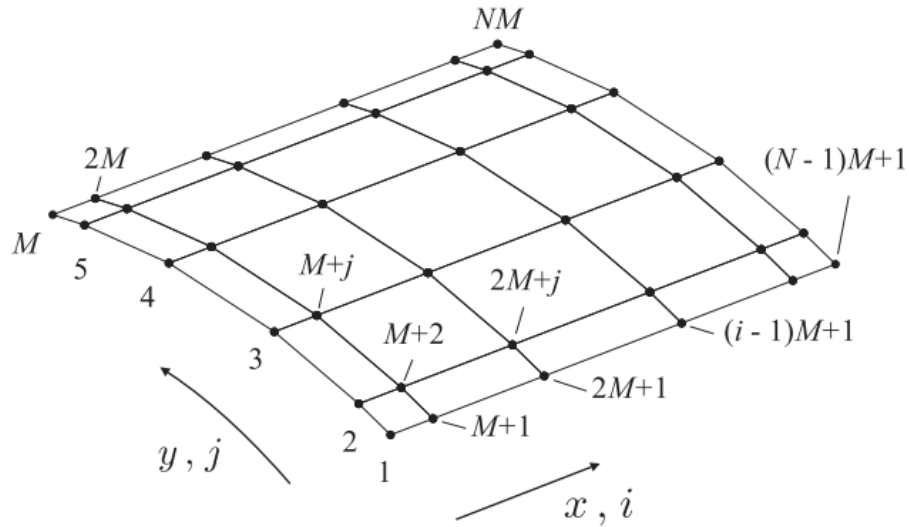


Fig. 12 A non-uniform 2D Chebychev-Gauss-Lobatto grid.

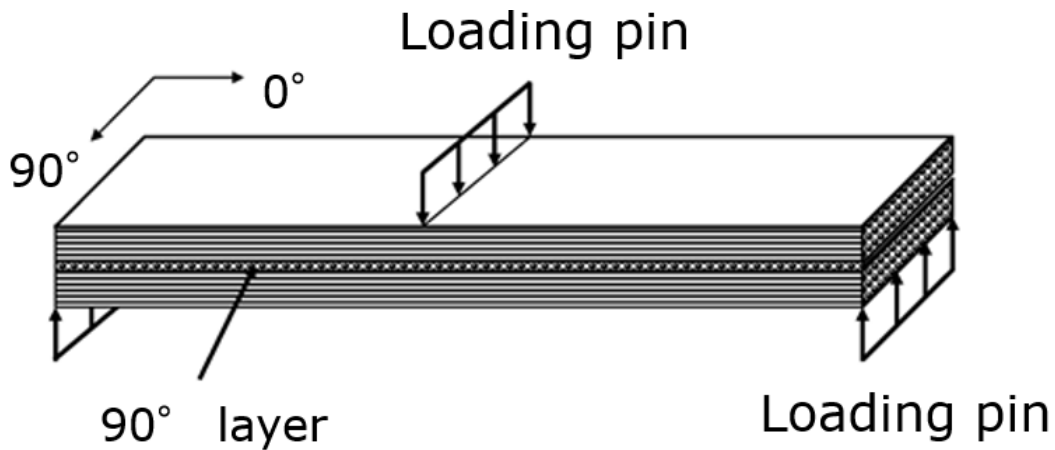


Fig. 13 The loading configuration of a laminated beam with two blocks of  $[0]_{12}$  and one 90-layer modeled and experimentally tested by Yuen et al. [13]. The 90-layer is either placed in a neutral central position creating a  $[0_{12}/90/0_{12}]$  laminate, or on the tension side for a  $[0_6/90/0_{18}]$  laminate, or on the compression side for a  $[0_{18}/90/0_6]$  laminate. These configurations are denoted by  $\frac{1}{2}$  beam,  $\frac{1}{4}$  beam and  $\frac{3}{4}$  beam, respectively. Different length beams of 40 mm, 48 mm and 56 mm were tested by Yuen et al. [13], and these results are treated as benchmarks herein.

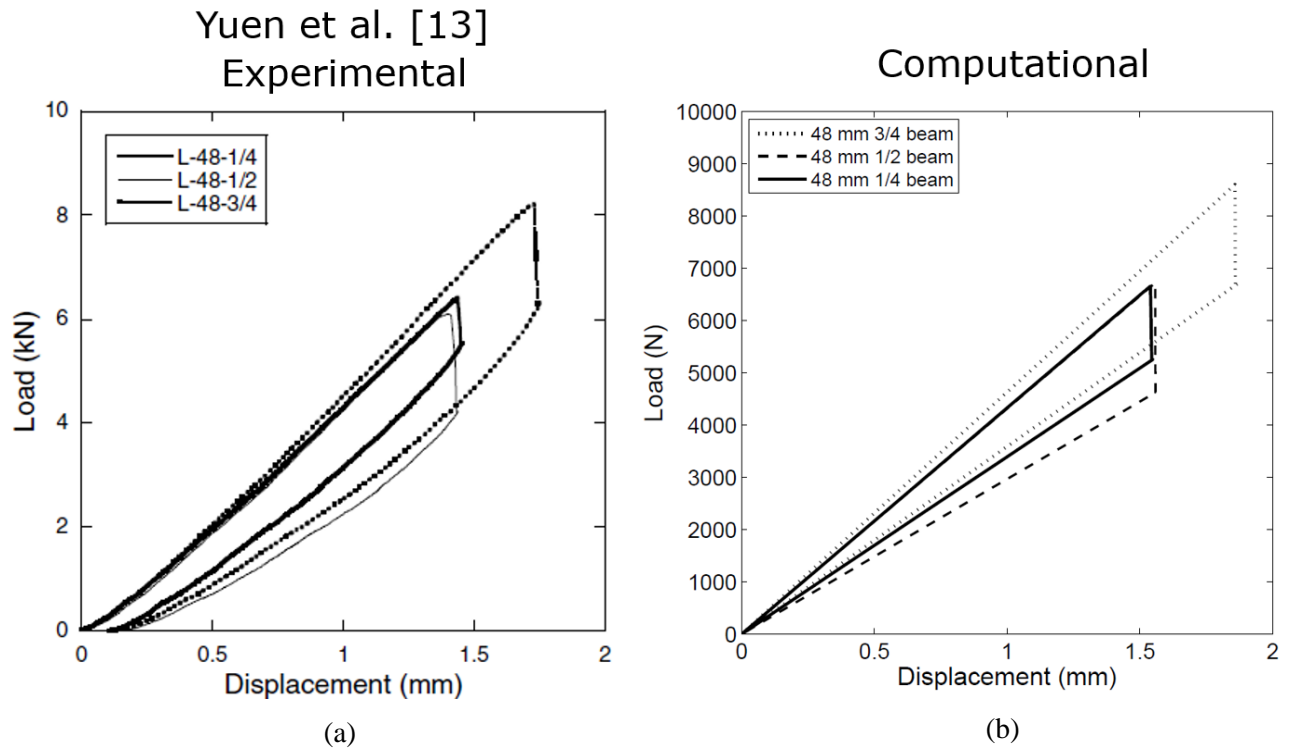


Fig. 14 Comparison of experimental results of 48 mm long beams by Yuen et al. [13] in (a) and the corresponding RZT beam computational results in (b).

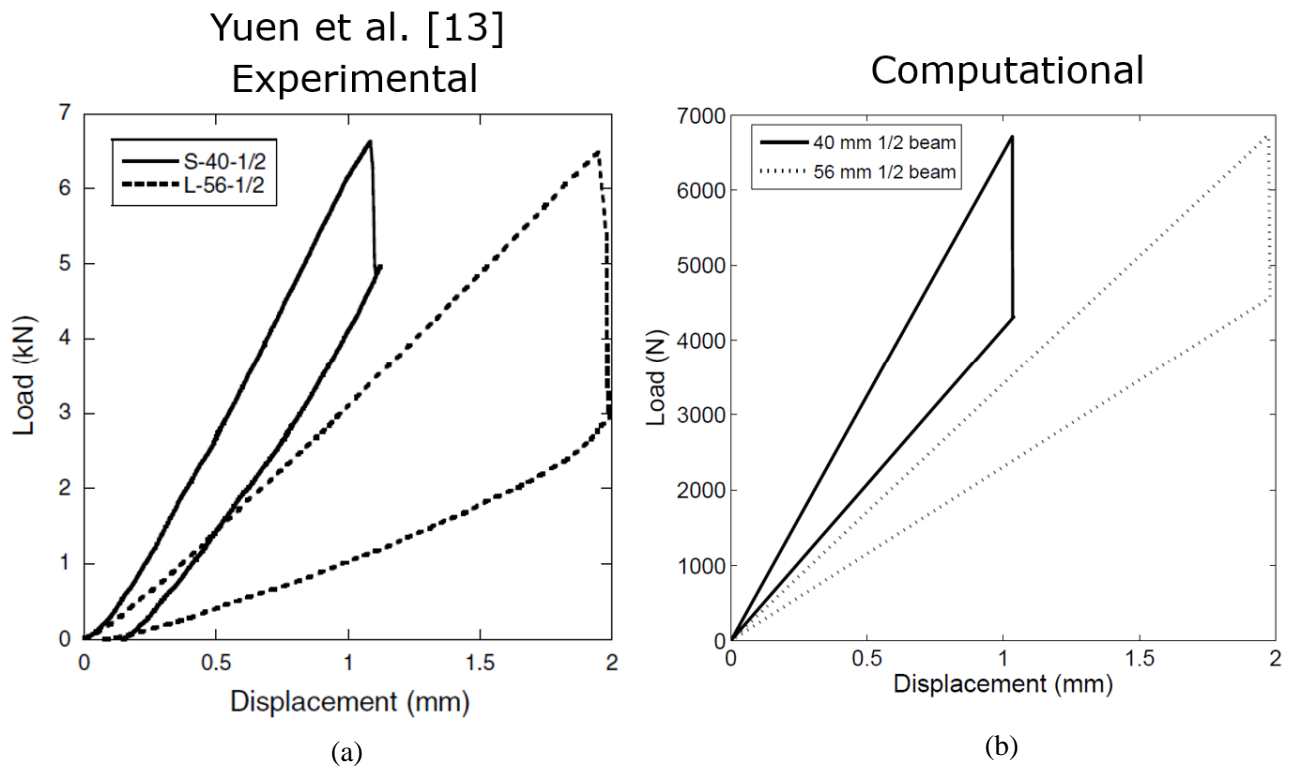


Fig. 15 Comparison of experimental results of 40 mm and 56 mm long beams by Yuen et al. [13] in (a) and the corresponding RZT beam computational results in (b).

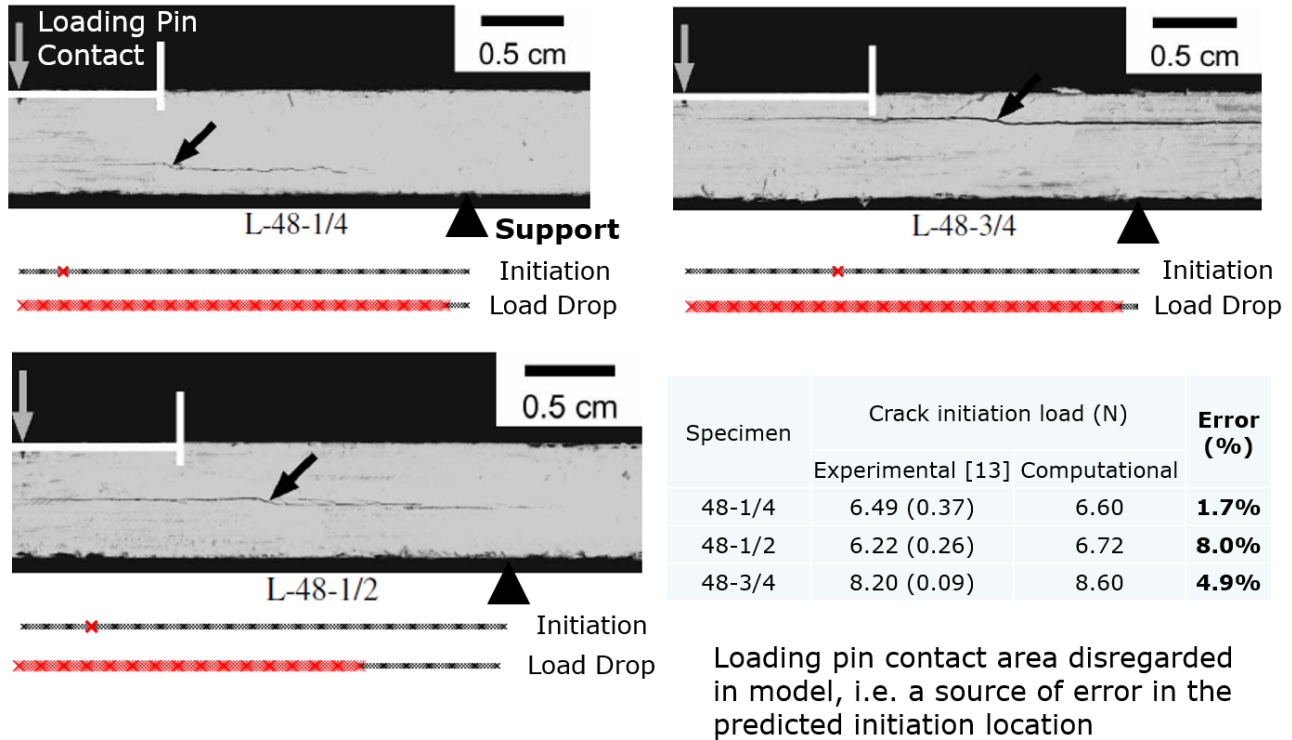


Fig. 16 Comparison of the initial delamination initiation site and final propagation length of experimental results by Yuen et al. [13] and the present RZT results. The table shows the percentage error in predicting the crack initiation load.

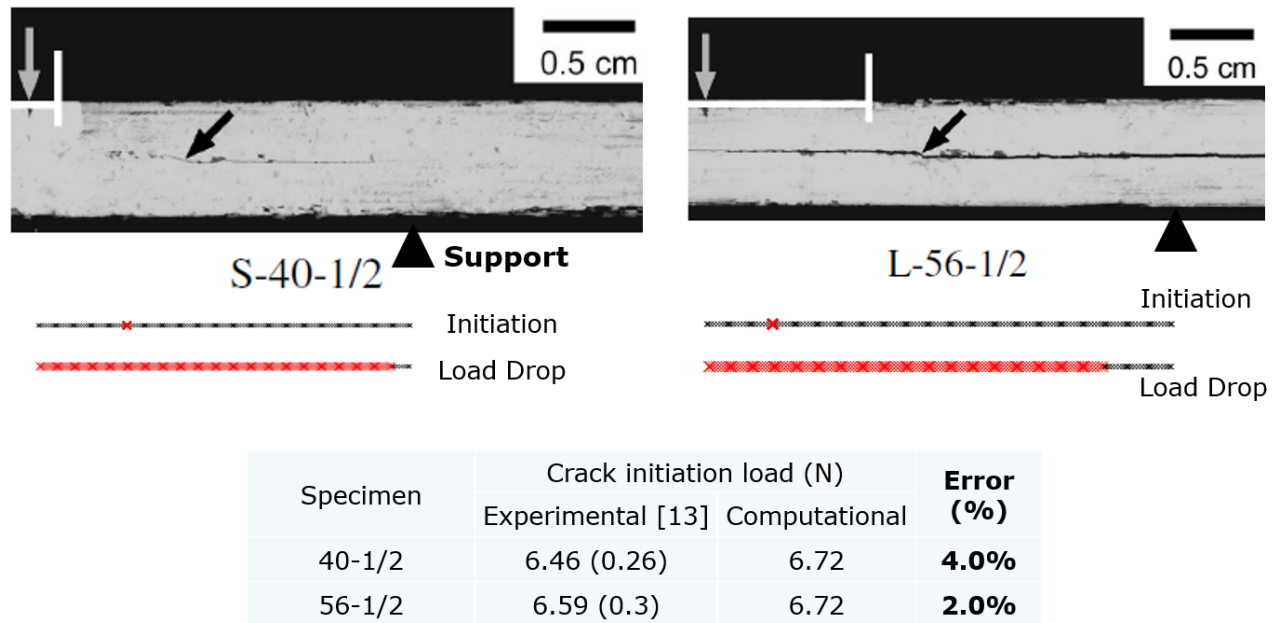


Fig. 17 Comparison of the initial delamination initiation site and final propagation length of experimental results by Yuen et al. [13] and the present RZT results. The table shows the percentage error in predicting the crack initiation load.

REPORT DOCUMENTATION PAGE			Form Approved OMB No. 0704-0188		
<p>The public reporting burden for this collection of information is estimated to average 1 hour per response, including the time for reviewing instructions, searching existing data sources, gathering and maintaining the data needed, and completing and reviewing the collection of information. Send comments regarding this burden estimate or any other aspect of this collection of information, including suggestions for reducing this burden, to Department of Defense, Washington Headquarters Services, Directorate for Information Operations and Reports (0704-0188), 1215 Jefferson Davis Highway, Suite 1204, Arlington, VA 22202-4302. Respondents should be aware that notwithstanding any other provision of law, no person shall be subject to any penalty for failing to comply with a collection of information if it does not display a currently valid OMB control number.</p> <p><b>PLEASE DO NOT RETURN YOUR FORM TO THE ABOVE ADDRESS.</b></p>					
1. REPORT DATE (DD-MM-YYYY) 01-10-2015		2. REPORT TYPE Technical Memorandum		3. DATES COVERED (From - To)	
4. TITLE AND SUBTITLE Application of the Refined Zigzag Theory to the Modeling of Delaminations in Laminated Composites			5a. CONTRACT NUMBER		
			5b. GRANT NUMBER		
			5c. PROGRAM ELEMENT NUMBER		
6. AUTHOR(S) Groh, Rainer M.; Weaver, Paul M.; Tessler, Alexander			5d. PROJECT NUMBER		
			5e. TASK NUMBER		
			5f. WORK UNIT NUMBER 826611.04.07.01		
7. PERFORMING ORGANIZATION NAME(S) AND ADDRESS(ES) NASA Langley Research Center Hampton, VA 23681-2199			8. PERFORMING ORGANIZATION REPORT NUMBER  L-20610		
9. SPONSORING/MONITORING AGENCY NAME(S) AND ADDRESS(ES) National Aeronautics and Space Administration Washington, DC 20546-0001			10. SPONSOR/MONITOR'S ACRONYM(S)  NASA		
			11. SPONSOR/MONITOR'S REPORT NUMBER(S) NASA-TM-2015-218808		
12. DISTRIBUTION/AVAILABILITY STATEMENT Unclassified - Unlimited Subject Category 39 Availability: NASA STI Program (757) 864-9658					
13. SUPPLEMENTARY NOTES					
14. ABSTRACT The Refined Zigzag Theory is applied to the modeling of delaminations in laminated composites. The commonly used cohesive zone approach is adapted for use within a continuum mechanics model, and then used to predict the onset and propagation of delamination in five cross-ply composite beams. The resin-rich area in-between individual composite plies is modeled explicitly using thin, discrete layers with isotropic material properties. A damage model is applied to these resin-rich layers to enable tracking of delamination propagation. The displacement jump across the damaged interfacial resin layer is captured using the zigzag function of the Refined Zigzag Theory. The overall model predicts the initiation of delamination to within 8% compared to experimental results and the load drop after propagation is represented accurately.					
15. SUBJECT TERMS  Cohesive law; Continuum damage model; Delamination; Failure modes; Laminated composites; Refined zigzag theory					
16. SECURITY CLASSIFICATION OF:			17. LIMITATION OF ABSTRACT	18. NUMBER OF PAGES	19a. NAME OF RESPONSIBLE PERSON
a. REPORT	b. ABSTRACT	c. THIS PAGE			STI Help Desk (email: help@sti.nasa.gov)
U	U	U	UU	22	19b. TELEPHONE NUMBER (Include area code) (757) 864-9658